REDUCING SAMPLE STAGE DRIFT VELOCITY

High-contrast imaging in transmission electron microscopes requires that thermal drift of the sample stage is minimised. For this, the use of a Kalman filter strategy within the control structure of the stage has been investigated. A Kalman filter requires a thermal model of the stage construction, various inputs, and temperature measurements. In conjunction with a deformation model, this technique can compensate for drift. The compensation control strategy has been validated using simulations based on multiple measurements.

MARJOLEIN DAANEN

Introduction

Technology will always be evolving. Future-generation machines must be faster, while the accuracy must increase. Machines such as microscopes, milling machines and pick-and-place machines are examples of this. Currently, the accuracy of these machines is often limited by disturbances, resulting in effects such as thermal deformations.

Thermo Fisher Scientific is a leading manufacturer of transmission electron microscopes. These microscopes can create an image of a sample, down to the atomic scale. Creating such an image with picometer resolution requires high-precision technology. Hence, even the slightest disturbances deteriorate the quality of the images.

In the case of this article, the sample manipulation stage positions the sample in a microscope in three degrees of freedom. Its sub-nanometer position accuracy is affected by thermal deformations, mainly caused by variations in ambient temperature and internal heat loads generated by actuators and sensors in the stage. Temperature changes of millikelvins cause thermal deformations in the order of nanometers, resulting in undesired sample movement, known as drift. For confidentiality reasons, the geometry of the stage cannot be disclosed in this article and some quantities are only presented as normalised values.

To allow high-contrast imaging in the microscope, high exposure times are used. However, with long exposure times, the drift velocity – in the order of nm/min – will cause significant motion blur. By shortening the exposure time, the motion blur is reduced, but so is the contrast. The key to have both high contrast and little motion blur is to reduce the drift. Hence, to create an image with high contrast and good quality, the motion blur – and thus the drift – should be reduced. Figure 1 shows two images with

AUTHOR'S NOTE

Marjolein Daanen graduated on the subject of this article from Fontys Engineering University of Applied Sciences in Eindhoven (NL) in 2021. For this, she received a nomination for the Wim van der Hoek Award. She now is an M.Sc. student in Systems & Control at Eindhoven University of Technology and lecturer of Mechatronics at Fontys.

marjoleindaanen@hotmail.com

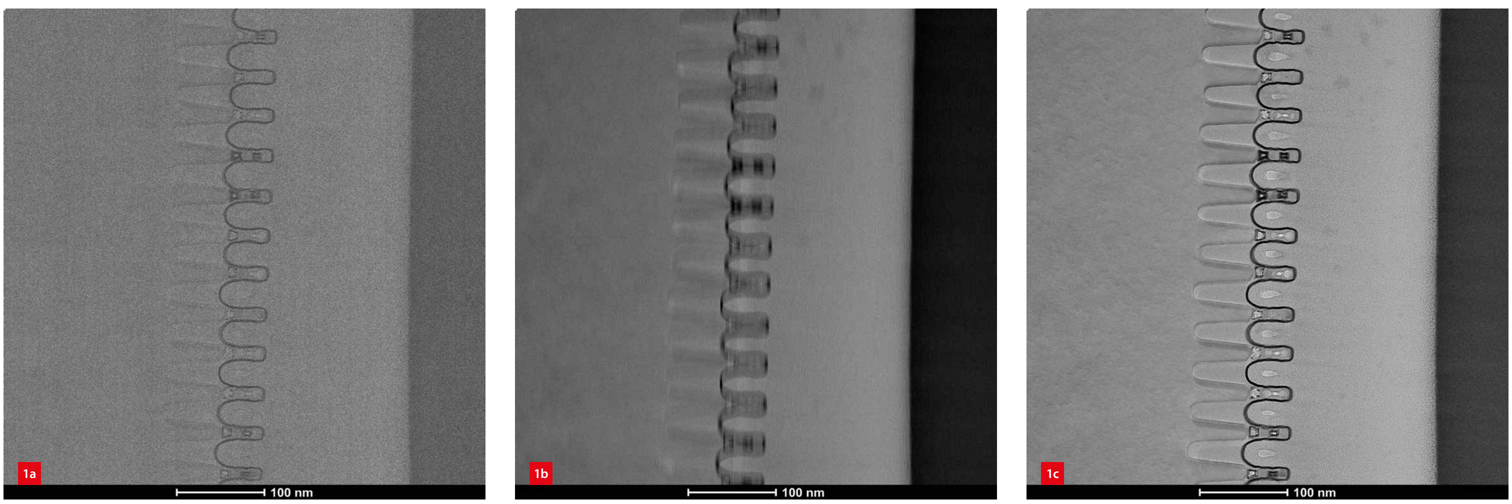

Three images of the same nano-wire sample.
(a) Low contrast.
(b) Motion blur.
(c) Good quality.

either low contrast or motion blur, and one of sufficient quality. To acquire images with sufficient quality, the drift velocity (normalised to the maximum allowable value) may – by definition – not exceed ±1.

The stage has been designed to fulfil various design requirements, such as high eigenfrequencies and high positioning accuracy. Although thermal effects have also been minimised, the current design still exhibits some thermal drift, which limits performance. At the same time, the thermal deformations cannot be measured. Therefore, the current stage controller cannot compensate for these disturbances.

Compensating technique

Although it is not possible to measure the thermal deformations, it is possible to measure the temperatures on various locations across the stage. In addition, the desired output of the actuator, which is a measure of the power dissipated in the actuator, and the ambient temperature can be measured. On top of that, the stage has a highly predictable thermomechanical behaviour. This allows modelling of the thermal deformations in the stage, based on the internal and external temperatures and heat loads.

Based on these findings, a new control structure design has been developed [1]. This structure aims to predict and compensate for thermal deformations caused by actuator dissipation, other internal heat loads, and ambient temperature variations. However, in this article the effects of actuator dissipation are out of scope.

For the new control structure, a thermal model has been developed, based on the lumped-element method (LEM). The main benefit of using this modelling technique over others is the low computational load, making fast simulations possible for real-time control. In addition, this method provides insight into the stage model. The details of this method are explained in the text box.

The developed model uses the desired actuator output, the estimated heat that is generated by sources, such as encoders, and the measured ambient temperatures to predict the temperatures of all the lumps representing the entire stage. In total, the thermal model contains around 200 lumps. A Kalman filter has been realised, which uses the thermal model in combination with temperature sensors. These sensors are strategically placed on the stage construction. Based on the temperature sensor readings, the Kalman filter allows real-time corrections to the thermal mode state estimations. This minimises the effect of modelling errors.

Continue on page 44

Lumped-element method

To create the thermal model of the stage, the lumped-element method (LEM) has been used. In this method, the geometric design of the stage is reduced to a set of discrete elements (lumps). Each lump has a certain thermal capacity and is connected to other lumps. Between these lumps, heat transfer takes place.

The heat transfer between the lumps is modelled by thermal resistors. Therefore, the model is a network of thermal resistors and thermal capacities, also known as an RC-network. Based on this RC-network, the temperatures over time of each thermal capacity (lump) can be found by solving a set of ordinary differential equations.

Model representation

Figure 2 visualises the two basic steps to create a LEM model from a simple block. The final model of this example consists of three thermal capacities (lumps), which are represented with the circles C_1, C_2 and C_3. The lumps are connected in series through resistors R_1 and R_2. Moreover, heat Q enters through lump C_1. Additionally, the resistors R_3, R_4 and R_5 connect the lumps to the ambient temperature, allowing to model convection and radiation.

Biot number

Using the LEM, each lump is assumed to have a homogeneous temperature. To ensure this, the Biot number (*Bi*) [2] is used to confirm the construction of the lumps. *Bi* describes the ratio between the internal thermal resistance (related to internal conduction) and the external thermal resistance (related to convection and radiation) of the lump. If $Bi < 0.1$, the temperature at the centre of the lump will not differ more than 5% from the temperature at the surface of the lump, and hence the lump geometry concerned can be used. The *Bi* value can be found using:

$$Bi = R_{\text{internal}} / R_{\text{external}} = l_c / (\lambda A_t) \cdot hA_t / 1 = l_c h / \lambda$$

Here, l_c is the characteristic length V/A_t, where V represents the volume of the body in [m^3], A_t represents the heat transferring area of the body in [m^2], λ represents the thermal conductivity of the body in [W/(mK)] and h represents the convective heat transfer coefficient in [W/(m^{2}K)].

Model parameters

In the LEM model, the following parameter values are determined for each lump:
- thermal capacity C [J/K];
- thermal conductive resistance R_{cond} [K/W];
- thermal convective and radiative resistance R_{comb} [K/W].

The thermal capacity C of each lump is found by:

$$C = c_p V \rho$$

Here, c_p is the specific heat capacity of the material in [J/(kgK], V is the volume of the body in [m^3] and ρ is the density of the material in [kg/m^3]. The volume of the body is obtained by the 3D CAD model of the lump. The specific heat capacity and the density of the material that the lump is made of can be found in literature.

The thermal conduction between the lumps is determined by performing a finite-element analysis, where a temperature $\Delta T = 1$ °C is applied between two points. From this analysis, the heat flow Q in [W] can be determined. Based on the equation below, this heat flow is the inverse of the thermal resistance R_{cond} in [K/W]:

$$R_{cond} = \Delta T / Q$$

In the LEM model, the convection and radiation heat transfer coefficients h_{conv} and h_{rad}, respectively, are linearised because the ambient temperature varies around 21 °C within a small range of ±2 °C. Linearisation allows combining both phenomena in a single coefficient. This combined heat transfer coefficient h_{comb} in [W/m^{2}K)] can be described as:

$$h_{comb} = h_{conv} + h_{rad}$$

This combination results in a heat flow:

$$Q = (T_l - T_{amb}) / R_{comb}$$

Here, resistance $R_{comb} = (h_{comb} \cdot A_{comb})^{-1}$, where A_{comb} is the heat transferring surface area in [m^2], T_l is the temperature of the lump in [K], and T_{amb} is the ambient temperature in [K].

For each lump, the ordinary differential equation is equal to:

$$C\dot{T} = \Sigma Q$$

Here, C is the thermal capacity of the lump, $\dot{T}$ is the time derivative of the temperature of the lump, and Q represents the various heat flows into the lump, defined positive if it increases the temperature of the lump.

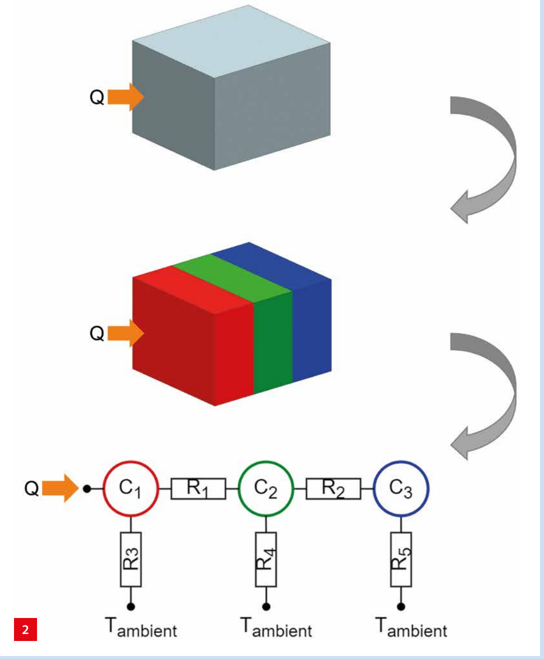

2

The two basic steps to create a LEM model from a simple block with a heat input Q. In step 1, the block is divided into three lumps. In step 2, the actual model is shaped, where Q enters the first lump, represented by thermal capacity C_1. The thermal capacities C_1, C_2 and C_3 are connected to each other through resistors R_1 and R_2. Finally, each thermal capacity is connected to the ambient temperature through resistors R_3, R_4 and R_5, enabling convection and radiation modelling.

Kalman filter

If the states of a system cannot be measured directly, such as the temperatures in the stage, a state observer can be used in control theory. A state observer estimates all the – observable – internal states of a real system. This is achieved by creating a mathematical model of the system and using the known inputs and outputs of the system. In case of the thermal model used for this application, the states are equal to the temperatures in the model.

A Kalman filter (KF) is a type of state observer designed for stochastic systems. In the control structure as described in this article, a thermal model in combination with the actuator output results in a prediction of all the internal states. The KF combines this prediction with the real-time temperature sensor data, to find the optimal estimation of the states. With this combination, the filter benefits of both methods (modelling and measuring), resulting in a higher accuracy and reliability of the estimation.

When the internal states are estimated using only a model, any model mismatch or unmodelled dynamics will create an error between the estimation and reality. This error can result in an estimation that, over time, will deviate from reality. If the internal states are estimated only based on measurements, sensor noise will introduce an error. Secondly, the number of sensors is limited for practical reasons and costs. While sensor noise is typically fast, the typical behaviour of a thermal system is slow, which makes a KF ideal for thermal system applications.

A KF involves a two-step process; see Figure 3. The first step is the so-called prediction step. During this step, the model predicts the observable internal states, as described before. In the second step, the prediction is updated, based on the sensor data; this is called the update step.

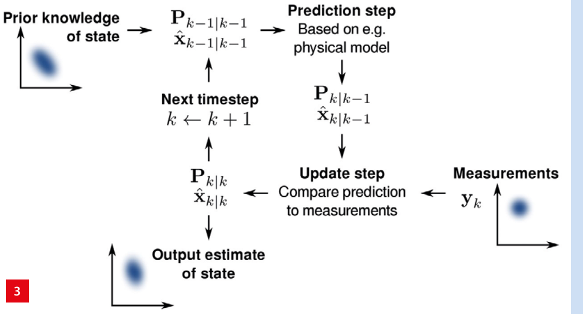

3

A basic flowchart describing the working principle of a Kalman filter. $\hat{x}_{k|k-1}$ denotes the estimate of the system's state x at time step k before the k-th measurement y_k has been taken into account; $P_{k|k-1}$ is the corresponding uncertainty. (Source: Petteri Aimonen, Wikipedia)

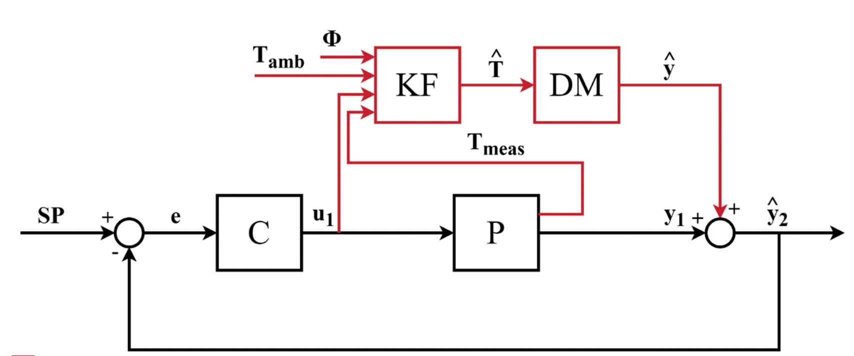

4

The control structure that is used to compensate for thermal deformations in the stage, where the black diagram represents the original control loop and the red diagram represents the added control loop.

Together with a deformation model, produced from the geometry of the stage and the material properties of the used materials, an estimation of the thermal deformations can be made. With this estimation, the error in the sample position – caused by thermal deformations – can be predicted and thus compensated for. More detailed information about the theory of a Kalman filter is given in the text box.

The control structure as described previously is shown schematically in Figure 4. The original control loop for the stage, containing the controller (C) and plant (P) representing the stage, is shown in black. The added control path, consisting of components for the Kalman filter (KF) and the deformation model (DM), is shown in red.

The inputs and outputs of these blocks are defined as follows:

- SP represents the position setpoint of the sample in [m];
- e represents the sample positioning error in [m];
- u_1 represents the desired output of the actuator in [rad/s];
- T_{meas} represents the measured temperatures on the stage in [K];
- T_{amb} represents the measured ambient temperature in [K];
- Φ represents all the additional signals – such as prior knowledge about sensor heat load – required to estimate the temperatures across the set-up;
- $\hat{T}$ represents the estimated temperatures of all the lumps in the stage in [K];
- $\hat{y}$ represents the estimated deformation of the stage in the actuating direction in [m];
- y_1 represents the measured position of the stage in [m];
- $\hat{y}_2$ represents the estimated position of the stage in [m].

The predicted temperatures of each lump from the KF are used to estimate the corresponding deformations in the stage. These estimated deformations can be determined by the equation that describes the relation between a deformation and a temperature change of a lump:

$$\Delta l(t) = \Delta T(t) \cdot \alpha \cdot l_{eff}$$

Here, $\Delta l(t)$ is the change in length over time in [m], $\Delta T(t)$ is the change in temperature over time in [K], α is the coefficient of thermal expansion (CTE) in [K^{-1}], and l_{eff} is the effective length of the lump in the deformation direction in [m]. Here, the deformation of a lump is assumed to be equal in all directions.

The CTE α is a general material property and can be assumed to be a constant, since the stage construction temperatures vary within a small range of ±2 °C around the average ambient temperature. The values for the CTEs are obtained from literature. The effective length l_{eff} of a lump is determined by the geometric length of the lump in the direction that affects the total stage deformation. In this way, each 3D lump is reduced to a 1D length. The effective length of each lump is determined using the 3D CAD model of the stage. By linearly summing all individual estimated deformations of all lumps in the stage, the total deformation of the stage can be estimated.

Controller validation / Results

Because the KF uses the thermal model for predictions, the model needs to represent the reality as accurately as possible in order to minimise errors. Therefore, multiple measurements on a stage set-up have been conducted. The measured ambient temperatures were used as inputs to a simulation, using only the thermal model, resulting in the model-based estimation of the temperatures in the set-up. The estimation was then compared to the actual temperature measurements on the set-up to obtain a measure of the errors in the model.

During a measurement of 20 hours, the ambient temperature varied within 1.8 °C, as can be seen in Figure 5. The measured temperatures in the set-up also varied within this range. Throughout this measurement, the actuator was not set in motion. The error between the temperatures

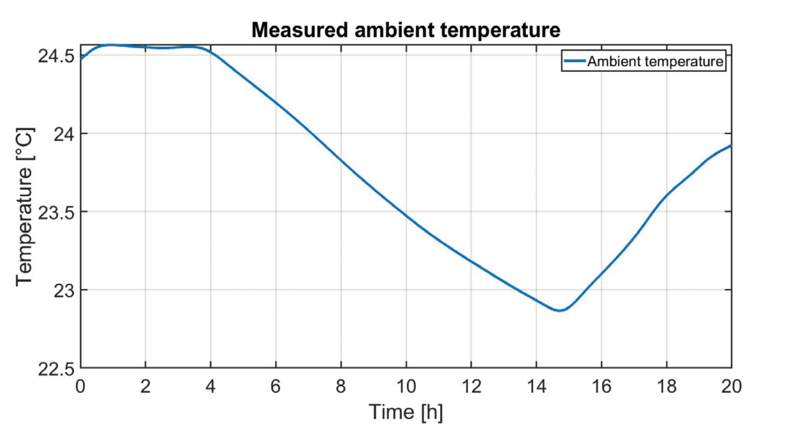

5

The measured ambient temperature around the stage.

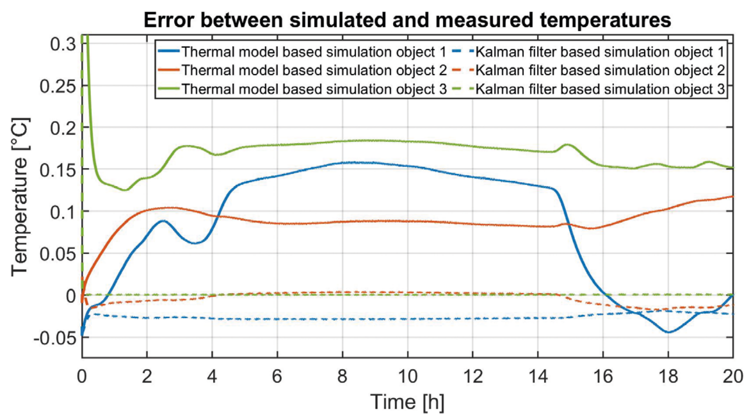

6

The error between the simulated temperatures, based on either the thermal model or the Kalman filter, and the measured temperatures for three selected lumps (objects 1 to 3).

of three selected lumps predicted by the simulation of the set-up, and the actual measured temperatures is shown with solid lines in Figure 6. In the first 2.5 hours, transient behaviour from the initial states to the estimated states was observed for the error based on the thermal model. In the remaining hours, the errors were within a range of ±100 mK with a maximum offset of 175 mK.

Note that around 3.5 h and 14.5 h, the temperature errors started varying. It is expected that this is caused by the constant heat transfer coefficient that is assumed within the model. In reality, this coefficient can vary in the range of 3.5 to 8 W/(m^{2}K). When the ambient temperature variation changes direction, this can cause an error in the thermal model. The measurements showed these ambient temperature direction changes around 3.5 h and 14.5 h. At the same time, the errors started varying, which can be seen in Figure 6.

Also in Figure 6, the effect of the KF can be seen. Using the same measurement as before, the temperature estimation error using the KF is shown using the dotted lines. These results demonstrate that the KF improves the temperature estimation significantly. The offset of the estimated temperatures has been reduced from 175 mK to a maximum of 30 mK. In addition, the temperature error variation has been improved from a maximum of ±100 mK to ±15 mK. Comparable results were obtained from the other measurements.

Using a dedicated test set-up, it was possible to measure the deformation of the stage at the point of interest for validation purposes. The final predicted deformation that was achieved – based on the earlier given temperature estimations – as well as the measured deformation, is shown in Figure 7. Both deformations are normalised and within the nanometer range. In the first hour of the simulation, transient behaviour was apparent. In the remaining time, the simulated deformation showed similar behaviour as the measured deformation. However, when the ambient temperatures changed direction – around 3.5 h and 14.5 h – the simulated deformation responded immediately to this change, whereas the measured deformation exhibited the effect of a much larger time constant.

Simulations showed comparable results using other datasets. Hence, this error (the deviation of simulation results from measurements) could be caused by unmodelled thermal dynamics with different time constants, which would affect the deformation induced by ambient temperature variation significantly. Most likely, a combination of unmodelled thermal dynamics and the assumed constant heat transfer coefficient as mentioned before, could have led to the deformation error.

Figure 8 shows the normalised drift velocity that occurred with and without compensation, based on the predicted deformation that could be achieved so far. In the first hour, transient behaviour was observed – indicated by the grey area. In the remaining hours, the system with compensation showed a reduction of a factor 3.5 in normalised drift velocity as long as the ambient temperatures had a constant gradient (between 4.2 h and 14.4 h).

When the ambient temperatures changed direction, around 3.5 h and 14.5 h, the compensated drift velocity was equal or slightly less than the drift velocity without compensation and the goal (i.e. normalised drift velocity within ±1) was not met. A possible explanation can be found in the modelling error that arose when the ambient temperature changed direction.

The reduction factor over the entire time range was found to be 2. In total, the drift velocity without compensation was inside the target range for 17% of the time – indicated by the orange area. The compensation technique reduced the drift velocity such, that the time the drift velocity

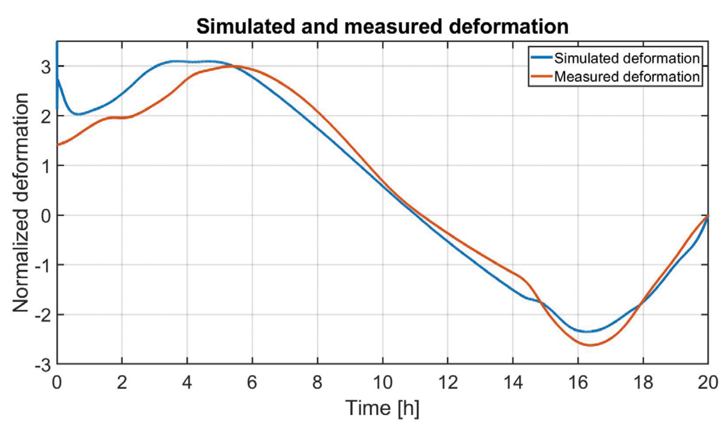

7

The total simulated (predicted) and measured deformation.

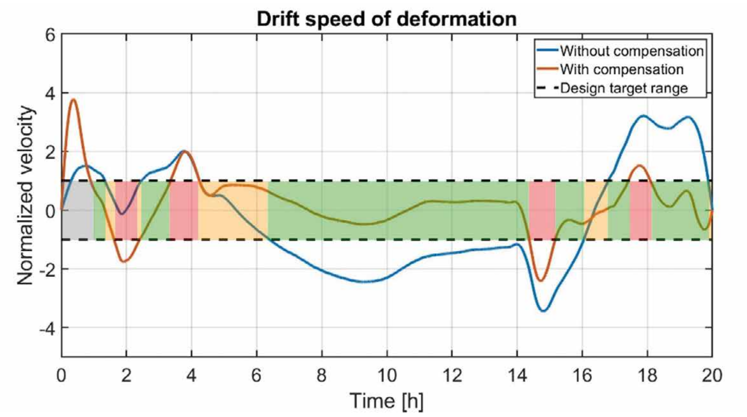

8

The normalised drift velocity with and without compensation. The grey area shows the time when transient behaviour occurred. The green area (67%) shows the time when the velocity based on compensation was within the target range whereas the velocity without compensation was not. The orange area (17%) shows the time when the velocity was within the target range both with and without compensation. The red area (16%) shows the time when the velocity was not within the target range both with and without compensation.

was within the target range increased to 84% – indicated by the orange and green areas.

Conclusion

The aim of this project was to investigate whether drift can be reduced to the design target range by using a Kalman filter strategy within the control structure of the stage. Drift is caused by thermal deformations due to varying ambient temperatures and heat generated by actuators and sensors within the stage. The control technique used in this case employed a Kalman filter, which requires a thermal model of the stage construction, various inputs, and temperature measurements. In conjunction with a deformation model, this technique can compensate for drift.

The compensation control strategy has been validated using simulations based on multiple measurements. The objective of the project was to compensate for drift to obtain a normalised drift velocity within a range of ±1. During a 20-hour measurement in which no actuator was moved, the ambient temperature varied within a range of 1.8 °C. For this data set, the normalised drift velocity without compensation was within the design target range of ±1 for 17% of the time. Applying the compensation control technique reduced the normalised drift velocity such that the design target range was met for a total of 84% of the time.

The factors that most likely limited the performance of the compensation are assumed to be errors in the model, such as spatially and temporally varying parameters within the model, such as convection. Also, unmodelled dynamics could result in lesser performance. It is conjectured that with further research into these errors, and with more optimisation, the desired design target for the normalised drift velocity can be met. Lastly, additional research is required to validate the effect of the actuator on the results. It has been proven that the compensation technique can be used to reduce the normalised drift velocity. Moreover, this technique offers enough room for improvement and boosting its performance. All things considered, the compensation technique shows promising results in reducing drift velocity.

REFERENCES
[1] M. Daanen, "Thermal drift compensation – The implementation and realization on a three degrees of freedom sample manipulation stage", B.Sc. thesis, Fontys Engineering University of Applied Sciences, Eindhoven (NL), 2021.
[2] T.W. Davies, "Biot number", *Thermopedia*, *www.thermopedia.com/content/585*